Nanocrystalline Metal Oxides as Unique Chemical Reagents/Sorbents

Erik Lucas, Shawn Decker, Abbas Khaleel, Adam Seitz, Shawn Fultz, Aldo Ponce, Weifeng Li, Corrie Carnes, and Kenneth J. Klabunde*[a]

Abstract: A new family of porous inorganic solids based on nanocrystalline metal oxides is discussed. These materials, made up of 4–7 nm MgO, CaO, Al_2O_3, ZnO, and others, exhibit unparalleled destructive adsorption properties for acid gases, polar organics, and even chemical/biological warfare agents. These unique sorption properties are due to nanocrystal shape, polar surfaces, and high surface areas. Free-flowing powders or consolidated pellets are effective, and pore structure can be controlled by consolidation pressures. Chemical properties can be adjusted by choice of metal oxide as well as by incorporating other oxides as monolayer films.

Keywords: adsorption · metal oxides · nanostructures

WHAT ARE NANOSCALE PARTICLES?

Figure 1. Size of nanostructured materials compared with atoms and with bulk solids.

The properties that change in the nanoregime include bandgaps (for semiconductors),[3] magnetic moments (for ferro- and ferrimagnetics),[4] specific heats,[5] melting points,[6] surface chemistry,[7] and morphology/particle shape.[8] For consolidated nanoparticles, metal pieces can be harder, and ceramic pieces can be more plastic than normal materials made from microcrystal-polycrystal consolidation.[9, 10]

Introduction

Nanostructured materials have attracted the attention of scientists,[1] engineers, and even politicians.[2] What is the reason? What is all the shouting about? Essentially, the reason is that nanocrystals in the 1 to 10 nm range make up a new realm of matter in which physical and chemical properties change as size changes (Figure 1). Although it is still difficult to understand the property changes in a theoretical sense, this phenomenon presents enormous opportunities for advances in science and technology. Contemplating that any nanostructured solid material can have variable properties based simply on size essentially makes the periodic table of the elements "three dimensional". Actually the potential new materials based on nanostructure are even broader than the solid elements of the periodic table; metal oxides, metal sulfides, tellurides, arsenides, bimetallics, and of course metals themselves need to be considered.

Metal Oxides in Nanocrystalline Form

Oxides of many metals possess very high lattice energies and melting points due to their high ionicity. In theory very small crystals of material with high lattice energies should be stable and resistant toward melting, atom/ion migration, and subsequent crystal growth, even at elevated temperatures. Therefore, if synthetic techniques to produce nanocrystals of highly ionic metal oxides were available, it should be possible to isolate and store these ultrafine materials. Furthermore these solids can exist with numerous surface sites with enhanced surface reactivity, such as crystal corners, edges, or ion vacancies (Figure 2).[8, 11, 12] Residual surface hydroxides can also add to the rich surface chemistry exhibited by metal oxides such as MgO, CaO, SrO, BaO, Al_2O_3, TiO_2, Fe_2O_3, ZnO, and others, and this chemistry is generally attributable to Lewis acid, Lewis base, and Bronsted acid sites of varying coordination, that is, metal cations, oxide anions, and surface −OH which can be isolated or lattice bound (Figure 3).

Indeed, in recent years it has been possible to produce nanocrystalline metal oxides of MgO, CaO, ZnO, and others by specially designed sol-gel or aerogel processes.[7, 13, 14] Their study as adsorbents and catalysts had led to two important discoveries: 1) surface reactivates are inherently higher per

[a] Prof. K. J. Klabunde, Dr. E. Lucas, Dr. S. Decker, Dr. A. Khaleel, A. Seitz, S. Fultz, A. Ponce, Dr. W. Li, Dr. C. Carnes
Department of Chemistry, Kansas State University
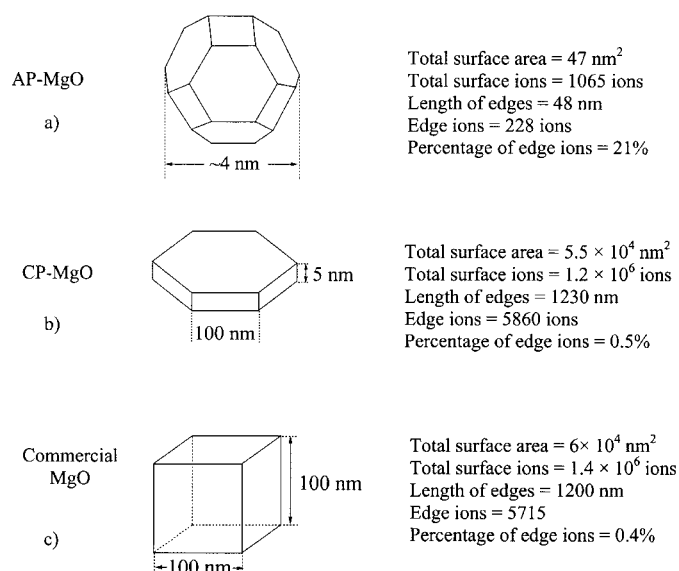Manhattan, KS 66506 (USA)
Fax: 785-532-6666
E-mail: kenjk@ksu.edu

AP-MgO
a)

~4 nm

Total surface area = 47 nm^2
Total surface ions = 1065 ions
Length of edges = 48 nm
Edge ions = 228 ions
Percentage of edge ions = 21%

CP-MgO
b)

5 nm
100 nm

Total surface area = 5.5×10^4 nm^2
Total surface ions = 1.2×10^6 ions
Length of edges = 1230 nm
Edge ions = 5860 ions
Percentage of edge ions = 0.5%

Commercial
MgO
c)

100 nm
100 nm

Total surface area = 6×10^4 nm^2
Total surface ions = 1.4×10^6 ions
Length of edges = 1200 nm
Edge ions = 5715
Percentage of edge ions = 0.4%

Figure 2. a) Model of MgO nanocrystal of polyhedral shape (AP-MgO); b) Model of MgO hexagonal microcrystal (CP-MgO); c) Model of cube-shaped microcrystal (CM-MgO).

Figure 3. Illustration of reactive surface sites on highly ionic metal oxides.

unit surface area for nanocrystals versus microcrystals, and 2) compaction of the nanocrystals into pellets does not significantly degrade surface area or surface reactivity when moderate pressures are employed,[8] ensuring that these nanostructured materials can be employed as very fine powders or as porous, reactive pellets. Figure 4 demonstrates that a loose powder of MgO compared with a pellet of compacted nano-MgO have similar pore structure. In fact the powder had a surface area of 343 m^{2}g^{-1} and possessed a total pore volume of 0.681 cm^{3}g^{-1}, whereas the values for the pellet was 331 m^{2}g^{-1} and 0.657 cm^{3}g^{-1}, respectively.[8] These interesting phenomena seem to be related to a fascinating aspect of nanocrystal formulation, that of shape of the nanocrystals.

Shape of Nanocrystals Affects Chemistry

Although the shape of crystals of a solid substance are of considerable beauty and curiosity, shape is not considered to
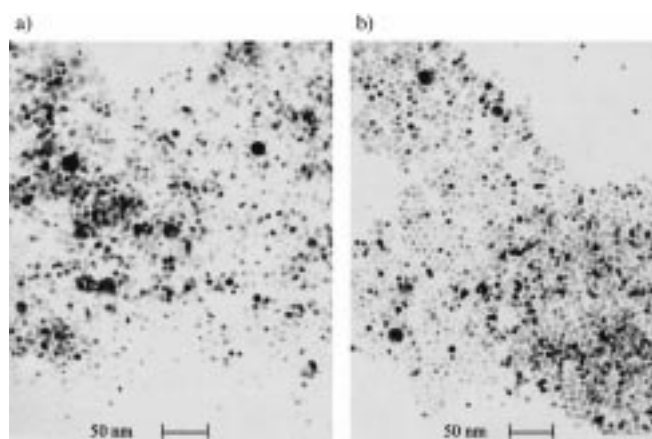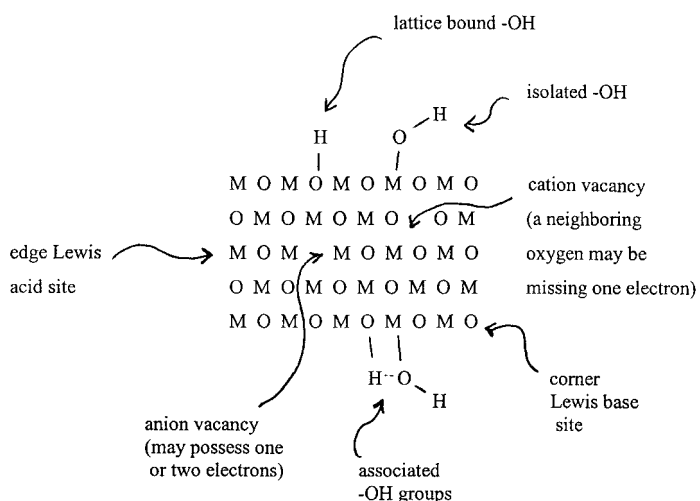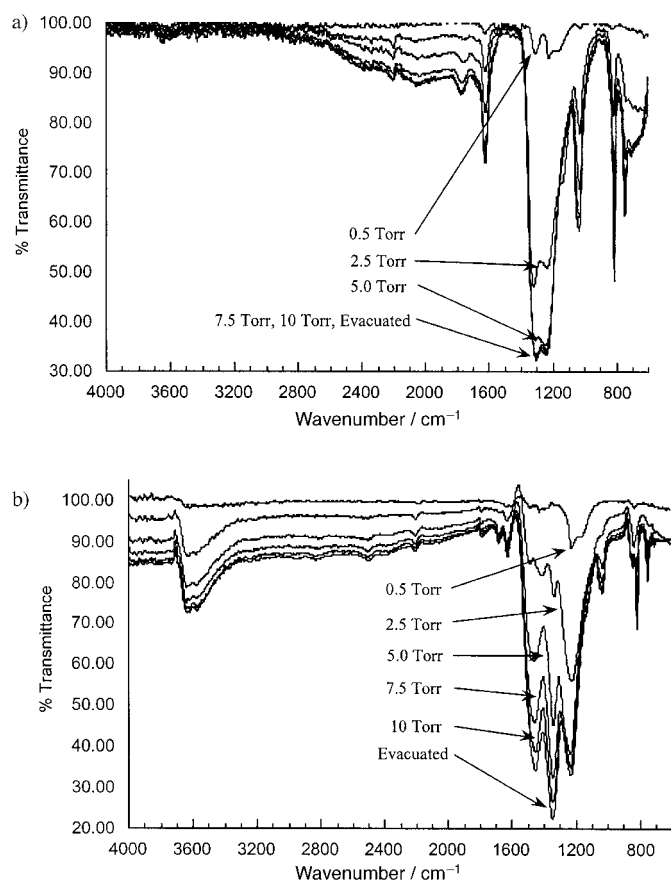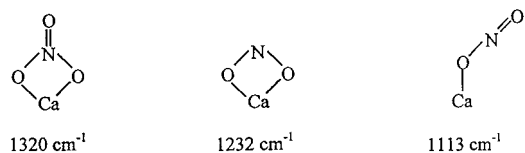

Figure 4. Transmission electron microscope picture of weakly agglomerated MgO nanocrystals a) compared with pellets b) produced by squeezing the MgO at 2.59×10^5 Torr. Note the evident pore structure.

have much effect on chemical properties. However, when crystals are in the 1–10 nanometer size range it appears that shape can affect chemistry. For example, 4 nm MgO crystallites adsorb six molecules of SO$_2$ per nm^2 at room temperature and 20 Torr pressure. However, microcrystalline MgO adsorbs only two molecule SO$_2$ per nm^2[15] Similarly, the nanocrystals adsorb four times as much CO$_2$ as the microcrystals. Beyond the differing amounts of adsorbed gases per nm^2, the mode of surface binding can be different, that is, SO$_2$ binds more as a monodentate species on the 4 nm MgO crystal, but favors a bidentate structure on the microcrystals.[15, 16]

These results clearly indicate that shape and size of crystals have remarkable effects on their adsorption properties. To what can this be attributed? As the models in Figure 2 indicate, the percentage of corner and edge sites on the surface of AP-MgO could approach 20%, while on CP-MgO less than 0.5%, and on CM-MgO essentially 0%. (Note: AP-signifies Aerogel Preparation that yields nanocrystals, CP-signifies an aqueous phase Conventional Preparation that yields microcrystals, and CM- signifies normal Commercially available polycrystalline materials). If adsorption on the edge sites were the predominant mode, it is easy to rationalize the experimental results. However, since the monolayer of SO$_2$ adsorbs tightly on the nanocrystalline surface, evidently much of the SO$_2$ must adsorb on flat plane areas as well.

Another system that has come under study is CaO, again in three different forms: 7 nm nanocrystals labeled as AP-CaO, microcrystalline hexagonal platelets labeled as CP-CaO, and larger cube-like common crystals labeled CM-CaO. After 500 °C heat treatment these crystals were exposed at room temperature to varying pressures of NO$_2$; the amounts adsorbed were determined by using a quartz spring microbalance and adsorption modes were studied by using a special cell for FTIR.[17] The IR results are shown in Figure 5. Note that for the nanocrystals of CaO (AP-CaO) peaks at 1232 and 1113 cm^{-1} grew in first at low pressures. As pressure increased, the peak at 1232 cm^{-1} became more intense, and then a strong peak at 1452 cm^{-1} appeared. The 1113 and 1452 cm^{-1} bands can be assigned to monodentate species, according to earlier

Figure 5. a) FTIR of NO$_2$ adsorbed on CP-CaO microcrystals; b) FTIR of NO$_2$ adsorbed on AP-CaO nanocrystals.

reports of NO$_2$ adsorption on MgO samples.[18] The strong bands at 1320 and 1232 cm^{-1} are assigned to bidentate adsorbed species (Scheme 1).

Scheme 1. Possible structures for NO$_2$ adsorption to a CaO surface.

The number of molecules of NO$_2$ adsorbed at 760 Torr at room temperature were 7 nm^{-2} for AP-CaO and 25 nm^{-2} for CP-CaO. These results were similar to those found for the SO$_2$/MgO system; this indicates that at low pressures the nanocrystals are much more effective adsorbents per unit surface area for strong chemisorption. However, at pressures above 100 Torr, multilayers form due to weak physisorption, and the flatter, more ordered CP-sample surfaces favor this physisorption due, apparently, to more ordered, tightly packed layers of SO$_2$ or NO$_2$.[15]

Both of these investigations show that shape and size of small crystals have profound effects on how much adsorption occurs and on the type of bonding to the surface that takes place. Since the nanocrystals are very small and are polyhedral spheroids, the fact that monodentate adsorption is preferred may indicate that the curvature of the crystallite

and/or the prevalence of the edge/corner sites encourages monodentate adsorption, whereas bidentate is favored by flat planes which are more prevalent on the larger microcrystals. Furthermore, the sequential growth of monodentate and then bidentate adsorption indicates that reactive edge/corner sites are occupied first, followed by the flat planes as pressure increases.

Somewhat similar behavior of nanocrystals has been found for CO adsorption on AP-MgO compared with CP-MgO and CM-MgO at low temperature. In fact, new IR bands for CO on AP-MgO suggest much stronger base sites, and these findings also indicate that size and shape of small crystals have significant effects on their adsorption properties. Although this may not be an unexpected conclusion, and the surface chemistry of crystals has been of interest for a long time,[19–22] the recent availability of nanocrystalline samples has allowed demonstration of vast differences due to crystal size and shape that had not been imagined before. Therefore, new and deeper understanding is required, which in turn suggests additional work.

Another approach to investigating the differences in surface reactivity of nano- versus microcrystals is to look at pH changes in water as a function of time. Solubility is slight for MgO (0.00062 g per 100 mL). It would be expected that upon placing a sample in cold water, the pH would rise to about pH 11. Since nanocrystalline MgO possesses a high surface area, usually in the range of 350–500 m^{2}g^{-1}, dissolution would be faster than with more conventional powdered samples (commercial MgO usually has a surface area of 30 m^{2}g^{-1} and a conventional preparation of microcrystalline MgO has a surface area in the range of 130 to 200 m^{2}g^{-1}).

Figure 6 shows plots of pH change versus time in which AP-MgO is aerogel-prepared nanocrystals, CP-MgO is conventionally prepared microcrystals, and CM-MgO is a commer-
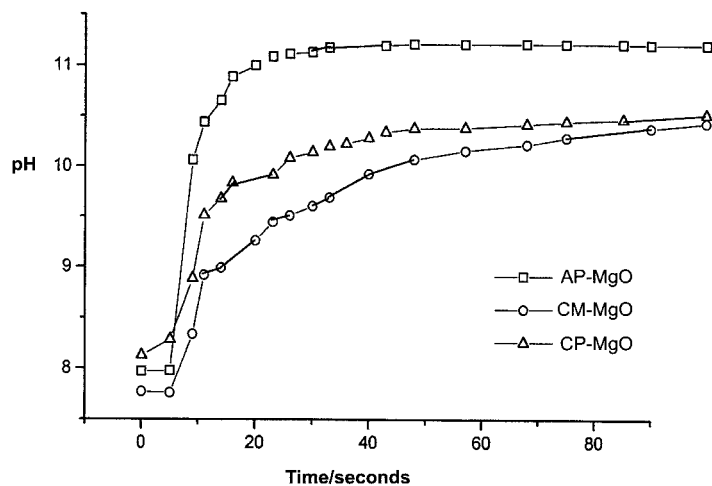

Figure 6. Rate of pH change for AP-MgO nanocrystals, CP-MgO microcrystals, and CM-MgO commercially available powder of relatively low surface area.

cially available sample. The rate of change can be computed as dpH/dt = pH change per second, and these values for a series of metal oxides are reported in Tables 1 and 2. It can be noted that MgO nanocrystals show an initial rate for driving

Table 1. pH change for MgO and CaO nano- and microcrystalline samples suspensions in cold water.

Metal oxide	Starting surface area (average) $[m^2 g^{-1}]$	pH after 10 s[a]	Initial rate [pH change per s]	Final pH
AP-MgO	350	10.9	0.53	11.0
CP-MgO	150	8.0	0.24	10.7
CM-MgO	30	8.3	0.27	11.0
AP-CaO	150	11.4	0.58	12.7
CP-CaO	50	11.8	0.62	12.7
CM-CaO	3	11.5	0.59	12.7
$[Fe_2O_3]$AP-MgO[b]	300	9.1	0.35	10.5
$[Fe_2O_3]$CP-MgO[c]	120	8.3	0.27	10.6
$[Fe_2O_3]$AP-CaO[d]	90	9.4	0.38	12.7
$[Fe_2O_3]$CP-CaO[e]	40	10.8	0.52	12.6

[a] Initial pH of deionized water was 5.6. [b] 2% loading as a coating of Fe_2O_3 on MgO nanocrystals. [c] 2% loading as a coating of Fe_2O_3 on MgO microcrystals. [d] 2% loading as a coating of Fe_2O_3 on CaO nanocrystals. [e] 2% loading as a coating of Fe_2O_3 on CaO microcrystals.

Table 2. pH change for suspensions of nano- and microcrystalline suspensions of ZnO, CuO, and Al_2O_3 in cold water.

Metal oxide[a]	Starting surface area (average) $[m^2 g^{-1}]$	pH after 50 s[b]	Initial rate [pH change per s]	Final pH
NC-ZnO	130	6.3	0.014	8.4
CM-ZnO	1.5	6.7	0.022	8.5
NC-CuO	135	6.4	0.016	7.5
CM-CuO	0.7	5.8	0.004	6.5
NC-Al_2O_3	790	7.0	0.027	7.4
CM-Al_2O_3	110	6.5	0.0018	6.8

[a] NC- signifies nanocrystalline, and CM- signifies commercially available polycrystalline material. [b] Initial pH of water was 5.6.

the pH up that is more than double that of more conventional powder samples. However, for CaO samples, a material that reacts strongly and exothermically with water to yield $Ca(OH)_2$ (which is more soluble in water than $Mg(OH)_2$), the initial rates are about the same for different samples. This can also be appreciated by observing the high final pH values.

Also of interest is that the initial rate of pH change can be slowed by coating the MgO or CaO particles with a very thin Fe_2O_3 layer, and these layered core/shell materials have proven especially effective in chlorocarbon destructive adsorption.[23]

Table 2 contains data on other nanosize metal oxide particles compared with commercially available powders. Mainly it should be noted that the initial rates are much slower and the final pH values considerable lower, which is expected of Al_2O_3, ZnO, and CuO.

Generally nanomaterials cause pH adjustments more rapidly than normal powders, and this is especially true for MgO and Al_2O_3. These results can be explained by surface area effects, and enhanced surface reactivity per m^2 is not indicated by these pH studies of powder samples. On the other hand, in destructive adsorption studies in which polar organic molecules are adsorbed, nanomaterials do exhibit inherently more active surfaces, and several examples are discussed below.
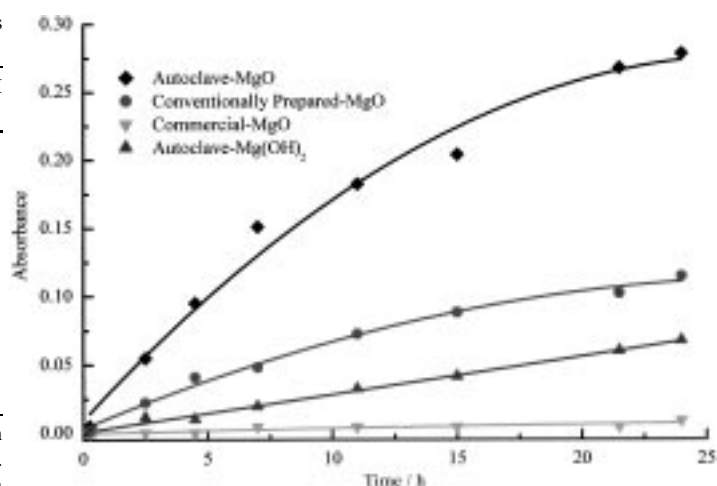
Figure 7. Rate of dehydrochlorination of 2-CEES ($CH_3CH_2SCH_2CH_2Cl$) by MgO nano- and microcrystalline samples at room temperature.

Acetaldehyde is adsorbed vigorously by AP-MgO. Compared with CM-MgO over the same time period, more than ten times as much acetaldehyde was adsorbed, and the initial rate was much higher.[24] The reaction of chloroethylethyl sulfide ($CH_3CH_2SCH_2CH_2Cl$, 2-CEES, a mimic of $ClCH_2$-$CH_2SCH_2CH_2Cl$, mustard gas) with AP-MgO, CP-MgO, CM-MgO, and AP-$Mg(OH)_2$ is shown in Figure 7 [see also Eqs. (1a) and (1b)][25] Normal MgO (CM-MgO) is completely unreactive, whereas the nanocrystals are highly reactive.

$$CH_3CH_2SCH_2CH_2Cl \xrightarrow{MgO} CH_3CH_2SCH=CH_2 + HCl \quad (1a)$$

$$2\,HCl + MgO \rightarrow MgCl_2 + H_2O \quad (1b)$$

There are numerous other examples. A particularly interesting one is the destructive adsorption of paraoxon (an insecticide and chemical warfare mimic) in pentane solution, in which AP-MgO is vastly superior to activated carbon samples both in rate and capacity (see Scheme 2).[26, 27]
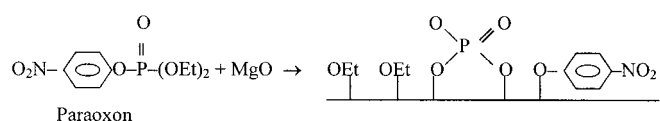
Scheme 2. Destructive adsorption of paraoxon.

AP-MgO strongly adsorbs a monolayer or about one molecule paraoxon per nm^2, whereas a typical activated carbon adsorbs about ⅕ of this per nm^2. Initial rates were also vastly different: 3.3×10^{-5} mol min^{-1} AP-MgO versus 0.28×10^{-5} mol min^{-1} for activated carbon.

We believe that this high adsorptive rate and high capacity are due to the polar nature of the metal oxide surface coupled with its reactive coordinately unsaturated surface (high percentage of edge/corner sites, vacancies, and other defects). However, another important reason is the accessibility of incoming adsorbates to the nanocrystalline surfaces. The nanocrystals actually exists as highly porous aggregates with large pore openings.

A question of some importance is: "can these great adsorbent properties be preserved after the nanocrystalline powders have been consolidated into hard, robust pellets (which is the likely form to be used in industry)?" Generally, the answer is yes, pellets can be formed and porous natured preserved, especially at low to moderate pressing pressures. In fact, pressure can be used to control pore structure, as shown in Table 3. Note that below about 2.59×10^5 Torr the pore

Table 3. Effects of compaction pressure on nanocrystalline MgO.

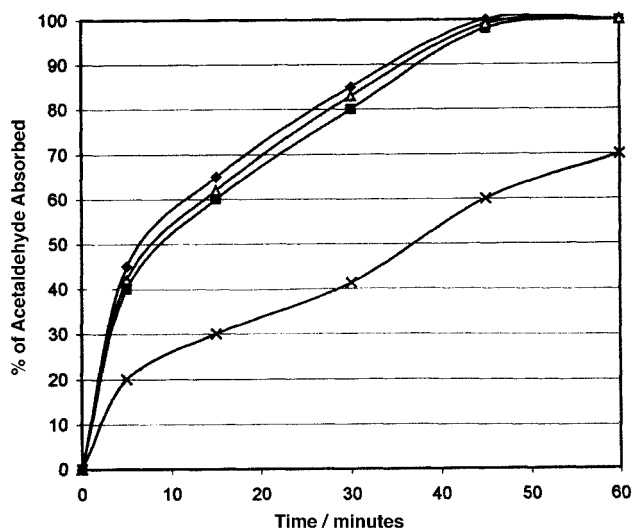| Load [$\times 10^5$ Torr]	Surface area [$m^2 g^{-1}$]	Total pore volume [$cm^3 g^{-1}$]	Average pore diameter [nm]
0	443	0.76	6.9
2.59	434	0.57	5.3
5.17	376	0.40	4.2
10.34	249	0.17	2.7

Figure 8. Rate of adsorption of acetaldehyde by nanocrystalline Al_2O_3 in powder or pellet form. The following pressures were used to compact and form the pellets at room temperature: $\blacklozenge$ = powder, $\blacksquare$ = 2.59×10^5 Torr, $\triangle$ = 5.17×10^5 Torr, $\times$ = 10.34×10^5 Torr.

structure remains relatively intact, and these pellets behave in adsorption processes essentially identical to the loose powders. For example, the rate and capacity of adsorption of methanol on pellets compressed at 0 (loose powder), 0.517×10^5, 1.034×10^5, and 2.59×10^5 Torr were nearly identical. However, pellets produced at 5.17×10^5 or 10.34×10^5 Torr were slower and less was adsorbed.[8]

There are other examples of powder–pellet comparisons in chemical processes and two are presented here. Returning to acetaldehyde, both nanoscale MgO and Al_2O_3 vigorously adsorb this aldehyde (with much higher rates and capacities than for activated carbon). The MgO or Al_2O_3 can be loose powder or compressed pellets. In a gas-recirculating reactor, containing acetaldehyde vapor mixed with air, the rate and capacity of adsorption of pellets and powder were measured; the results are shown in Figure 8. Note that only when very high compression pressure was used, was the adsorption process hindered.

modified as desired. It is also possible to load catalytic metals such that very high dispersions are possible, whereby the nanocrystalline oxide serves as an unusual catalyst support, for example Cu on ZnO.[29]

An often asked question about these new adsorbents is: "do they remain active in the presence of moist air?" The answer is affirmative for hours or days, but not months or years. Of course it depends on the specific application, for example, for the adsorption of aldehydes out of an air steam, 10 days prior exposure to room air did not significantly affect sorption properties of the nanocrystalline powder toward the aldehydes.[24]

Thus, there is great flexibility in design, and it would appear that nanocrystalline metal oxides represent a broad class of new porous inorganic materials.

Conclusion

It has been demonstrated that nanocrystalline metal oxides, especially MgO, CaO, Al_2O_3, and ZnO,[28] have unparalleled sorption properties for polar organics, acid gases, and other chemical species. Usually, destructive adsorption (dissociative chemisorption) takes place so that the target adsorbate is irreversibly destroyed. Unique morphological features (crystal shapes), pore structure, polar nature of the surfaces, and high surface areas are believed to account for these unusual sorption properties. Furthermore, these features can be maintained even after compression into pellets. Indeed, pore structures (pore volume and pore size openings) can be roughly controlled by compression pressure.

Since the oxide can be chosen for desired Lewis base/Lewis acid strengths, and since the oxides can be produced with thin layers of other chosen materials (e.g. Fe_2O_3, V_2O_3, Mn_2O_3, ZrO_2, etc.), surface chemical properties can be further

Acknowledgements

[1] K. J. Klabunde, C. Mohs in *Chemistry of Advanced Materials*: *An Overview* (Eds.: L. Interrante, M. Hampden-Smith), Wiley-VCH, New York, **1998**, pp. 271–327.

[2] Interagency Working Group on Nanoscience, Engineering, and Technology (IWGN) Workshop Report, *Nanotechnology Research Directions*, M. C. Roco, Chair, September **1999**, National Science Foundation Cooperative Agreement ENG-9707092.

[3] a) M. L. Steigerwald, L. E. Brus, *Acc. Chem. Res.* **1990**, *23*, 183; b) A. Henglein, *Chem. Rev.* **1989**, *89*, 1861.

[4] *Nanophase Materials*: *Synthesis, Properties, Applications* (Eds.: G. C. Hadjipanayis, R. W. Siegel), Kluwer, London, **1994**.

[5] H. J. Fecht, *Nanomaterials*: *Synthesis, Properties, and Applications* (Eds.: A. S. Edelstein, R. C. Cammarata), Institute of Physics, Philadelphia, **1996**, p. 105.

[6] a) T. P. Martin, U. Naher, H. Schaber, U. Zimmerman, *J. Chem. Phys.* **1994**, *100*, 2322; b) A. N. Goldstein, C. M. Euher, A. P. Alivasatos, *Science*, **1992**, *256*, 1425.

[7] K. J. Klabunde, J. V. Stark, O. Koper, C. Mohs, D. G. Park, S. Decker, Y. Jiang, I. Lagadic, D. Zhang, *J. Phys. Chem.* **1996**, *100*, 12142.

[8] R. Richards, W. Li, S. Decker, C. Davidson, O. Koper, V. Zaikovski, A. Volodin, T. Rieker, *J. Am. Chem. Soc.* **2000**, *122*, 4921.

[9] J. Karch, R. Birringer, H. Gleiter, *Nature*, **1987**, *330*, 556.

[10] R. P. Andres, R. S. Averback, W. L. Brown, L. E. Brus, W. A. Goddard, III, A. Kalder, S. G. Louie, M. Moscovits, P. S. Peercy, S. J. Riley, R. W. Siegel, F. Spaepen, Y. Wang, *J. Mater. Res.* **1989**, *4*, 704.

[11] M. Utiyama, H. Hattori, K. Tanabe, *J. Catal.* **1978**, *53*, 237.

[12] A. Pelmenschikov, G. Morosi, A. Gamba, S. Coluccia, *J. Phys. Chem.* **1995**, *99*, 15018.

[13] L. Ben-Dor, *Heterogenous Chem. Rev.* **1995**, *2*, 41.

[14] H. D. Gesser, P. C. Goswami, *Chem. Rev.* **1989**, *89*, 765.

[15] J. V. Stark, D. G. Park, I. Lagadic, K. J. Klabunde, *Chem. Mater.* **1996**, *8*, 1904.

[16] H. Itoh, S. Utamapanya, J. V. Stark, K. J. Klabunde, J. R. Schlup, *Chem. Mater.* **1993**, *5*, 71.

[17] O. B. Koper, I. Lagadic, A. Volodin, K. J. Klabunde, *Chem. Mater.* **1997**, *9*, 2468.

[18] L. Curruti, E. Modone, E. Guglielminotti, E. Borello, *J. Chem. Soc. Faraday Trans. I*, **1994**, *70*, 729.

[19] a) D. A. Sverjensky, *Nature*, **1993**, 364, 776; b) X. L. Zhou, J. P. Cowin, *J. Phys. Chem.* **1996**, *100*, 1055.

[20] J. M. Blakely, *Introduction to the Properties of Crystals Surfaces*, Permagon, New York, **1973**, pp. 7 – 10.

[21] a) A. W. Adamson, *Physical Chemistry of Surfaces*, 5th ed., Wiley, New York, **1990**, pp. 88 – 91, p. 382; b) E. Matijevic, *Langmuir*, **1994**, *10*, 8.

[22] a) I. Langmuir, *J. Am. Chem. Soc*, **1916**, *38*, 2221; b) B. M. Wechhuysen, G. Mestl, J. Lunsford, *J. Phys. Chem.* **1998**, *102*, 3773.

[23] A. Khaleel, K. J. Klabunde, D. Park, *High Temp. Mater. Sci.* **1995**, *33*, 99.

[24] A. Khaleel, P. Kapoor, K. J. Klabunde, *Nanostruct. Mater.* **1999**, *11*, 459.

[25] E. Lucas, Ph.D. Thesis, Kansas State University, **2000**.

[26] O. Koper, K. J. Klabunde, J. S. Klabunde, U.S. Patent, accepted and pending.

[27] O. Koper, M. J. Siegel, C. Mohs, S. Rajogopalan, S. Decker, S. Pates, D. Nichols, K. J. Klabunde, unpublished results.

[28] C. Carns, K. J. Klabunde, *Langmuir*, **2000**, *16*, 3764.

[29] C. Carnes, A. Ponce, unpublished results.